Numerical Study on Aeroacoustics Behaviour of Contra-Rotating Fans

Bukhari Manshoor[#1], Chia I Shin[#1], Djamal Hissein Didane[#1], Amir Khalid[*2], Muhammed Abdelfattah Sayed Abdelaal[+3]

[#]*Faculty of Mechanical and Manufacturing Engineering, Universiti Tun Hussein Onn Malaysia, MALAYSIA*
[*]*Faculty of Engineering Technology, Universiti Tun Hussein Onn Malaysia, MALAYSIA*
[+]*Engineers House Academy, Manshiet El Bakry Street, Qesm Heliopolis, EGYPT*

[1]bukhari@uthm.edu.my, [2]amirk@uthm.edu.my, [3]mohamed@engineers-house.com

Abstract - *The contra-rotating fan produces noise that can affect human health. Therefore, it is important to reduce the noise that is generated by the contra-rotating fan. In this research, the airflow performance and acoustic behaviour of the contra-rotating fan will be studied. The objectives of this study are to perform the simulations for the flow generation by the contra-rotating fans, furthermore, investigate the effect of the different spacing between the two propellers on the noise generation. The ANSYS Fluent with the RNG k-ε model was used to simulate the steady flow field of the fan, while Ffowcs Williams and Hawkings (FW-H) model was used to simulate the acoustic of the fan set. The simulation results show that the main source of the noise was from the fan propellers. The performance of the contra-rotating fan increases when the rotating speed of the propellers increases. However, it will also increase the noise. For the effect of distance between the two propellers, the noise generated by the contra-rotating fan decreases with the increase of the distance between the propellers. It can be concluded that with the suitable distance between the two propellers and rotating speed, the fan could function more efficiently while producing less noise.*

Keywords: *Aeroacoustic, Airflow, Contra-rotating fan, Noise, Sound pressure*

I. INTRODUCTION

Contra-rotating fans referred to the fan that contains two rotors rotating in opposite directions. This type of fan was widely used as a ventilation system of mine and other sites [1,2]. Currently, it is also mostly used use as a computer ventilation system due to the good performance to reduce the heat from the computer processor [3,4]. The contra-rotating fans have an advantage compare to the normal axial fan due to their capability to generate a straight and focused airflow. In some electronic devices, the requirements for small-sized fans with high rotational speed are very important for the efficiency of the device in heat release [5]. For that purpose, a contra-rotating fan is one of the choices that can overcome the problem of releasing big quantities of heat. Even though this type of fan has advantages compared to the normal axial

fans, it creates trailing edge noise due to the airfoil surface and the unsteady flow it interacts with [6,7]. The continuous noise that is generated by the fan can affect human health and make them feel uncomfortable [8]. Hence, it is important to understand the source of noise and aeroacoustics behavior to reduce the noise generated by the fan.

The noise generated by the fan is classified as aeroacoustics, which is a combination of noise from aerodynamic and mechanical vibration. The noise creates from the mechanical vibration mostly had been solving by active control noise. However, the contra-rotating fan which produces aerodynamic noise is more complicated where the noises are relatively high [9]. Currently, the difficulty was resolve by using the Computational Aeroacoustics (CAA) method that has obtained continuous improvements as well [10,11]. One of the interesting findings regarding the noise from the fan blade is it is mainly an aerodynamic noise, where the vibration noise can be negligible [9]. Simulation by using the CFD model and Ffowcs-Williams and Hawkings (FW-H) equation shows that the combination of CFD and CAA can be used to obtain the sound pressure due to the aerodynamics noise and at the same time prove that the vibration noise or structural noise can be negligible for aeroacoustics analysis. By using the method, Li *et al*. [12] used the Large Eddy Simulation (LES) with FW-H noise model to determine the effect of the various angles of an uncommon blade for axial fan performance. They found that the main noise sources are concentrated on the leading edge of the suction surface, and aerodynamic noise is generated by low-frequency sound.

According to the current study, the researchers found out the main source of the noise for contra-rotating fans is produced by the two propellers in the fan system [13,14]. Research by Wang etc. [15] found that the noise will be affected by the flow rate and distance between two propellers. Besides, another research claimed that the distance between two propellers would affect the efficiency of the fan [16]. As the distance between the propellers was increased, the efficiency of the fan will increase, then decrease after reaching a maximum. However, the previous work never discusses the effect of axial spacing on contra-

rotating fans on aeroacoustics yet. Hence, it is really necessary to determine the effect of axial spacing on contra-rotating fan on aeroacoustics performance.

This paper studied the performance and acoustic behavior using the CFD and FH-W equation to determine the effect of axial spacing of the contra-rotating fan. Based on the methods, the main purpose of this study is to perform the simulations for the flow generation by the contra-rotating fans, hence investigating the effect of the different spacing between the two propellers on the noise generation. The San Ace 172 model was taken as a reference in the model drawing. The numerical study was performed by using ANSYS Fluent software. The RNG k-ε model was used to simulate the steady flow field, and the FW-H model was used to simulate the acoustic of the fan. Then, the impact of axial spacing on the aerodynamic noises is analyzed.
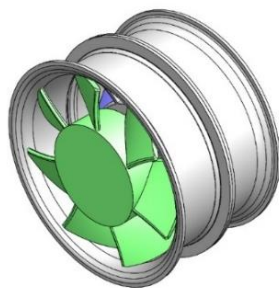
II. MODEL AND NUMERICAL SETUP

In this research, ANSYS Fluent software was used to perform the numerical simulation. The performance and acoustic behaviour of the contra-rotating fan were observed.

A. Model Setup and Meshing

The contra-rotating fan model used in this study is shown in Fig. 1. Basically, the model was referred to as the model of the SanAce 172 series contra-rotating fan model. The contra-rotating fan consists of 2 propellers, with the first propeller has 8 blades while the second propeller consists of 7 blades. The diameter for both propellers was 142 mm with 78 mm hub size in diameter and 28.5 mm width. The distance between the rotor and casing was 2 mm. The figure also illustrates the front and side view of both propellers.

The model for simulation is shown in Fig. 2. It consists of a cylindrical tube which is the domain of simulation and had been divided into five parts: inlet, rotor 1, the area between rotor 1 and rotor 2, rotor 2, and the outlet. The length of the cylindrical tube is 1000 mm with a 75.5 mm radius. The two rotors are placed in the center of the cylindrical tube.

First propeller – front and side view

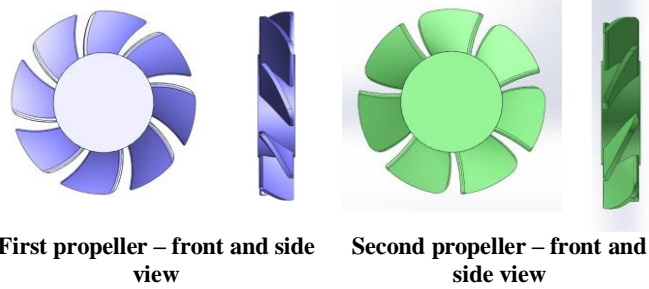**Second propeller – front and side view**
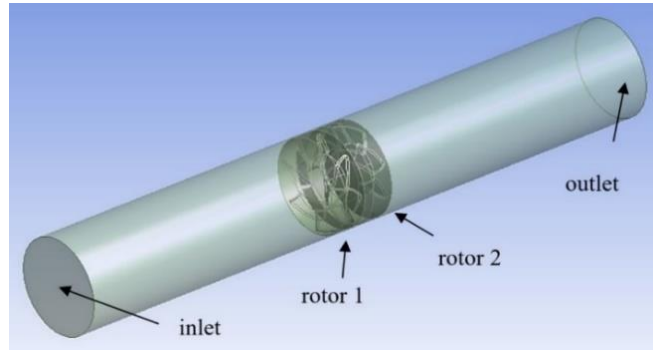
Fig. 1 Contra-rotating fan model

Fig. 2 Geometry domain and boundary condition

Meshing is a simulation process that discrete the complex geometry of the object into a simple element. It will affect the accuracy of the result by changing the element size. The smaller the value of the element size, the more accurate the value of the result. However, a finer element size needs more time to simulate the problem. In this study, the element size for the domain is 80 mm, while the element size for rotors is 0.9 mm. The purpose of this study is to observe the airflow performance of the contra-rotating fan, and hence, in order to get a more accurate result, a fine mesh element was used for the part of the rotors. The result of the meshing was shown in Fig. 3. The highest mesh skewness was lower than 0.89, as shown in Fig. 4.
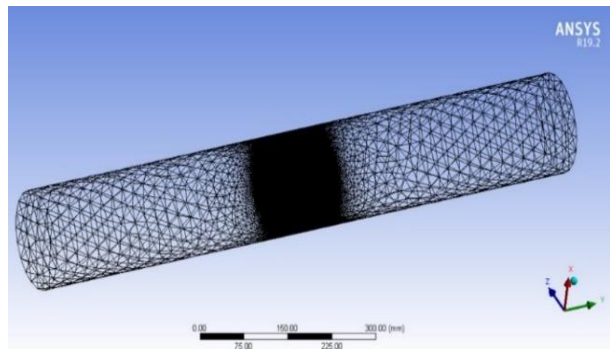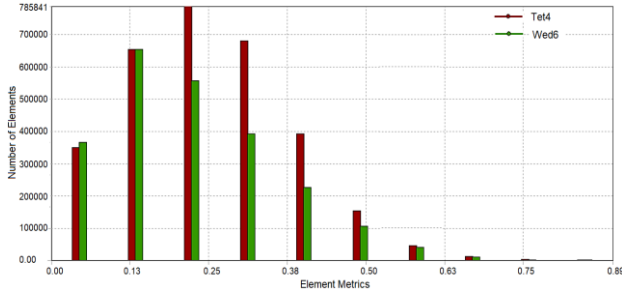

Set of contra-rotating fan

Fig. 3 Meshing

Fig. 4 Mesh skewness analysis

B. Numerical Setup

The RNG k-ε model was used in the simulation, and the wall boundary condition was set as a standard wall function. The RNG k-ε model was used to simulate the steady flow field of the fan system, and the results were taken as the initial field for unsteady flow. The model was set in converged, and all the parameters of residual were set at 10^{-5}. Table 1 shows the summarized parameters for the numerical setup.

Table 1 Model setup parameters for contra-rotating fan

Solver time Transient	Transient
Viscous model	RNG k-epsilon
Acoustic model	Ffowcs-Williams and Hawkings (FW-H)
Material	Air
Cell zone condition	Mesh motion
Rotation-axis direction	y
Rotational velocity	2000 rpm
Velocity-inlet	15 m/s
Propeller wall motion	Moving wall

The RNG k-ε model used a rigorous statistical technique to derive. There is an additional term in the RNG model's ε equation, which is able to improve the accuracy for rapid flow. Besides, it is able to analyze the low and Reynold number effects, unlike the standard model can only analyze for high Reynold number effects. Its features are more accurate and reliable compare to the standard k-ε model. The equation for RNG k-ε model show in the following equation 1.

$$\frac{\partial}{\partial t}(\rho k) + \frac{\partial}{\partial x_i}(\rho k u_i)$$
$$= \frac{\partial}{\partial x_j}\left(\alpha_k \mu_{eff} \frac{\partial k}{\partial x_j}\right) + G_k + G_b - \rho\varepsilon - Y_m + S_k \tag{1}$$

and

$$\frac{\partial}{\partial t}(\rho\varepsilon) + \frac{\partial}{\partial x_i}(\rho\varepsilon u_i)$$
$$= \frac{\partial}{\partial x_j}\left(\alpha_\varepsilon \mu_{eff} \frac{\partial\varepsilon}{\partial x_j}\right) + C_{i\varepsilon}\frac{\varepsilon}{k}(G_k + C_{3\varepsilon}G_b) \tag{2}$$
$$- C_{2\varepsilon}\rho\frac{\varepsilon^2}{k} - R_\varepsilon + S_\varepsilon$$

where,

G_b	Turbulence kinetic energy due to buoyancy
G_k	Turbulence kinetic energy due to the mean velocity gradients
Y_m	Fluctuating dilatation incompressible turbulence to overall dissipation rate
$\alpha_\varepsilon, \alpha_k$	Inverse effective Prandtl number for k and ε
S_ε, S_k	User-defined source terms

For the acoustic model, Ffowcs-Williams and Hawkings (FW-H) equation, or known as Lighthill acoustic analogy, is the most general equation to compute the acoustic field generated by the time-accurate flow computation [17]. The differential form of the FW-H equation is written as the following equation.

$$\frac{\partial}{a_o^2}\frac{\partial^2 p'}{\partial t^2} - \nabla^2 p' = \frac{\partial^2}{\partial x_i \partial x_j}\left[T_{ij}H(f)\right]$$
$$- \frac{\partial}{\partial x_i}\left\{\left[P_{ij}n_j + \rho u_i(u_n - v_n)\right]\delta(f)\right\} \tag{3}$$
$$+ \frac{\partial}{\partial t}\left\{\left[(P_o v_n) + \rho(u_n - v_n)\right]\delta(f)\right\}$$

where,

u_i	Fluid velocity component in the x_i direction
u_n	Fluid velocity component normal to the surface $f=0$
v_i	Surface velocity components in the x_i direction
v_n	Surface velocity component normal to the surface
$\delta(f)$	Dirac delta function
$H(f)$	Heaviside function

Equation (3) at the right-hand side needs to integrate over volume outside the data surface *f=0*, where the Lighthill stress tensor, T_{ij} is nonzero. The quadrupole term is neglected. With *f=0*, all the important noise sources on the surface will be located. Other than that, the integral form of the FW-H equation is written in acoustic pressure term with the contribution from monopoles (thickness noise), dipoles (loading noise), and quadrupole (flow fluctuation).

C. Setup Case

Two types of case studies were carried out in the research. The first case study is to observe the performance

and acoustic behavior of the flow and noise propagation by changing the distance between two rotors. The second case study was carried out by changing the turning speed of the rotors and the distance between the two propellers.

For the first case study, the axial spacing between two fan sets was changed, and it was running with the rotation speed at 2000 rpm for both propellers. The axial spacing between the two fan sets was 15 mm, 17.5 mm, 20 mm, 22.5 mm, and 25 mm, respectively. Next, for the second case study, the speed for both fans was changed; however, the distance between the two propellers remained constant, setting at 20 mm. The setting rotation for the propellers was 1300 rpm, 1650 rpm, 2000 rpm, 2350 rpm, and 2700 rpm. Meanwhile, the first propeller was rotated in a clockwise direction, and the second propeller was rotated in a contra-rotating direction so that it became a counter-rotating fan.

The following assumptions were made for the simulation work.

- The ambient background was in standard atmospheric pressure conditions.
- The gravity of gas and buoyancy were neglected.
- The airflow in the fan was turbulent.
- The airflow streamline was continuous.
- The inlet flow speed was set as 15 m/s.
- The moving reference frame will apply to the rotating rotors and stationary casing.

III. RESULT AND DISCUSSION

Several results will discuss in this section. The first result is the streamline for the flow across the counter-rotating fan. The next results that will be discussed are the velocity contour captured for the flow, and the last result for the flow behavior is the centerline velocity. For the aeroacoustic behavior, the results will discuss the sound pressure level obtained and also the broadband noise in terms of contour. The detailed discussion is in the next sections.

A. Streamline

Fig. 5 shows the streamline flow for different speeds of contra-rotating fans. As mentioned, the speed for the contra-rotating fan was set from 1300 to 2700 rpm for this study. The results for the streamlines were straight and narrow from the inlet until it almost reached the first propeller. It then followed the shape of the propellers and created a curve line until it reached the outlet. These results are as expected, and it shows that the simulation was converged very well. The results for the different distances between the rotor 1 and 2 were also analyzed from the simulation. The results show that the different distances did not give a significant effect on the streamlines. Therefore, the streamlined figures do not include in this paper for the simulation results.
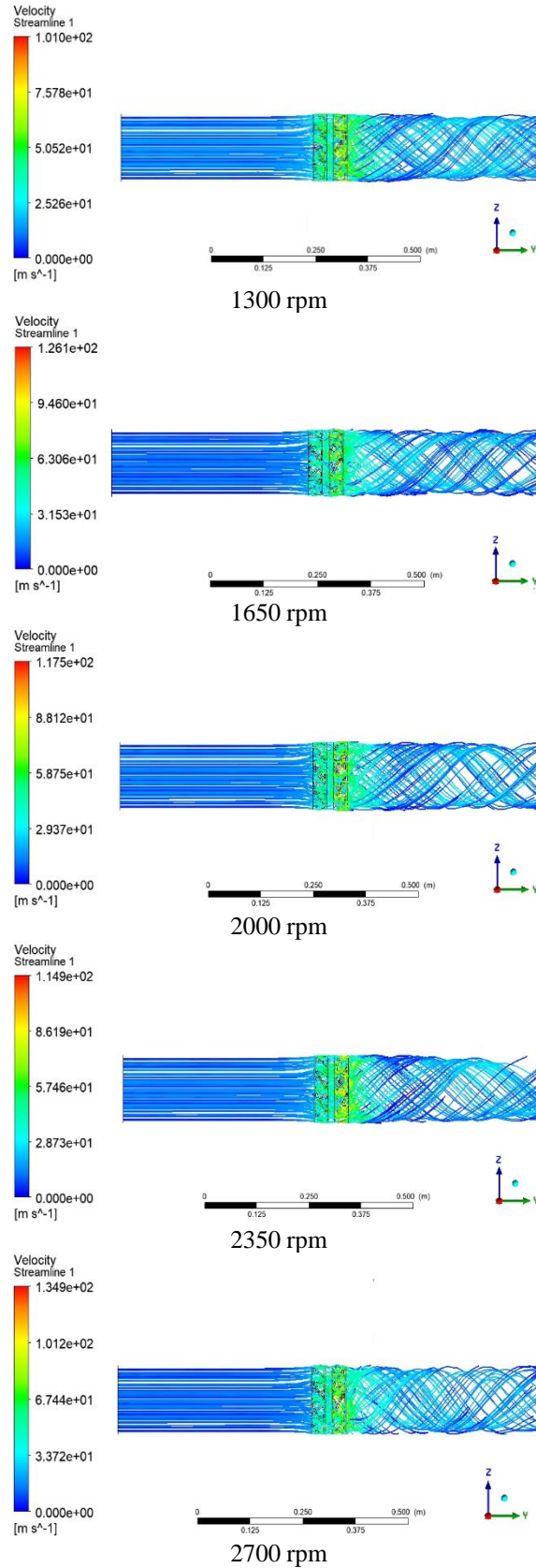

1300 rpm

1650 rpm

2000 rpm

2350 rpm

2700 rpm

Fig. 5 Streamlines for different speeds of the fan

B. Velocity Contour

For the velocity contour results with different distance between two propellers, 5 different distance was setup starting from 15 mm to 25 mm. Fig. 5 showed the results for the different setting. Discussion on the effect of distance between the two rotors, contra-rotating fan with 17.5mm distance between two propellers had the highest maximum velocity, which was 120.8 m/s, the second highest was 119.3 m/s with 15mm distance between two propellers, while 22.5 mm distance between 2 propellers had the lowest maximum velocity, which was 115.1 m/s. Besides, the maximum velocity for 20 mm and 25 mm were 117.4 m/s and 118.3 m/s. This showed that the distance between two propellers would affect the maximum velocity value.

The simulation also runs for different speeds of rotors, similar to mentioned before. The results show that the fan with the rotating speed of 1300 rpm had the highest maximum velocity, which was 165.4 m/s, the second highest was 134m/s with the rotating speed of 2700 rpm, while the rotating speed of 2350 rpm had the lowest maximum velocity, 115m/s. Besides, the maximum velocity for 1650 rpm and 2000 rpm were 126.1 m/s and 117.4 m/s. The results showed that the value of maximum velocity was not dependent on the rotating speed of the propeller. Although the fan set with 1300 rpm had the highest maximum velocity compare to other results, however, its overall velocity in the fan system was low.
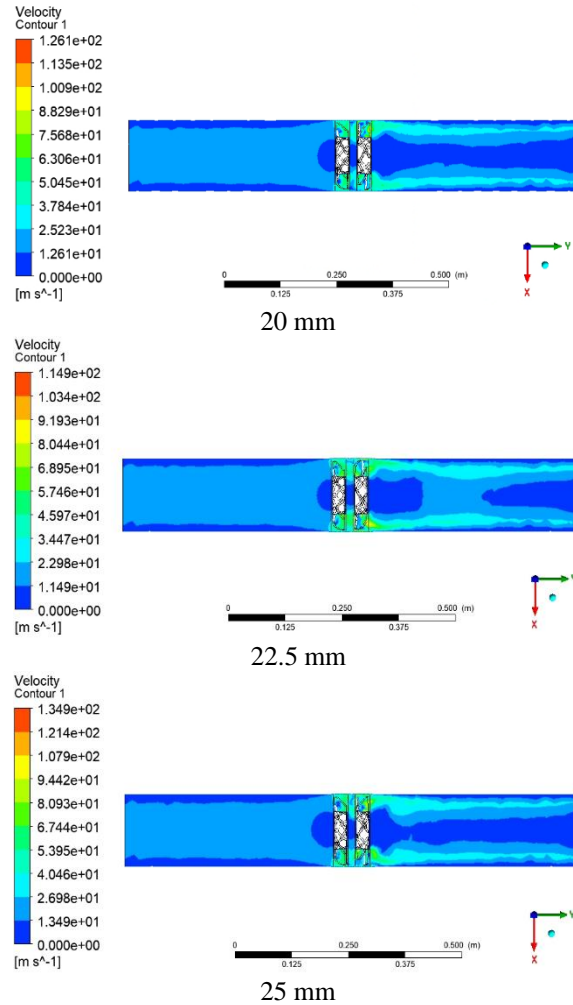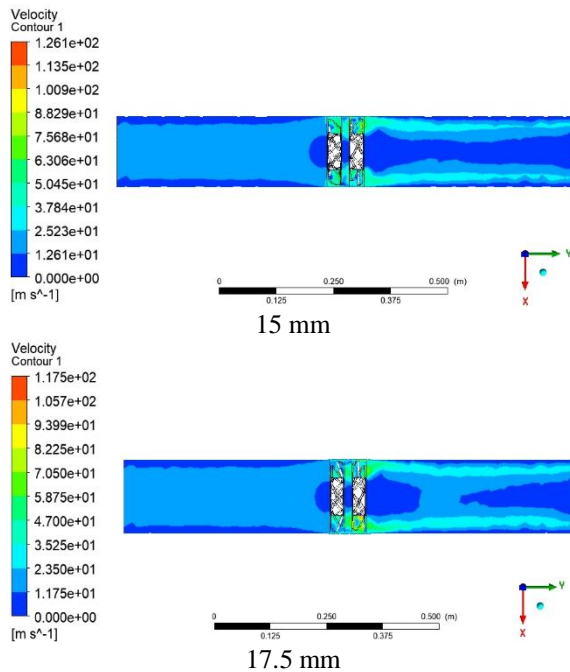

15 mm

17.5 mm

20 mm

22.5 mm

25 mm

Fig. 6 Velocity contour for a different set of the distance between two propellers

C. Centerline Velocity

The centerline was measure from the inlet to the outlet of the domain along the *y*-axis. With the 15m/s inlet speed, all the results from different settings produce the same pattern of the graph from the inlet to the first rotor. The centerline velocity started decreasing, approaching zero when the air flows across the first rotor. At the area between two rotors, the velocity increased and decreased when it reached a peak point. The highest peak point of the velocity between both rotors among those 5 results is 5.56 m/s, where its rotating speed is 1650 rpm. However, the highest peak point of the velocity after the second rotor among those 5 results is 25.8m/s, where its rotating speed is 2350 rpm. The centerline velocity downstream of the second rotor increasing as the distance is increased, and it is then decreased when it reached a peak point. The range of the peak points was located between 0.1 m and 0.3 m which is downstream of the second rotor. For the different speeds of rotors, the peak point for 1300 rpm, 1650 rpm, 2000 rpm, and 2700 rpm were 14 m/s, 14.5 m/s, 17.5 m/s, and 18 m/s,

respectively.

Fig. 7 shows the result of velocity magnitude at centerline for 5 the different setting speeds. From the figure, it shows that the fan set with 2700 rpm has the most constant velocity and has a higher velocity at the outlet. So, it has the best performance in this section.
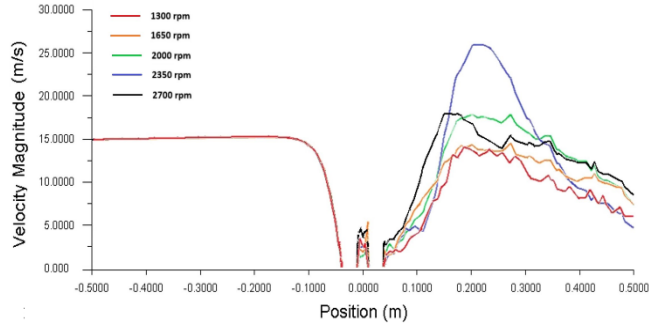

Fig. 7 Centerline velocity for a different set of speed

The results for the different distances between two rotors showed in Fig. 8. The results gave the same pattern of velocity from the inlet to the first rotor, which has 15 m/s constant velocities. The velocity starts to decrease and approaching zero when the air flows across the first rotor. At the area between two fan sets, the velocity increased and decreased when it reached a peak point. The highest peak point of the velocity between both rotors among those 5 results is 3.1m/s, where it has a 20 mm distance between two propellers. However, the highest peak point of the velocity after the second rotor among those 5 results is 23.75m/s, where the distance between two propellers is 25 mm. The graph for velocity downstream the second rotor increased as the distance increased, and it then decreased when it reached a peak point. The range of the peak points was located between 0.2 and 0.25m which is the area after the second fan set. The peak point for the distance between two propellers after the second fan set for 15 mm and 17.5 mm were 18m/s, while 20 mm and 22.5 mm were 17.8 m/s and 21 m/s, respectively. From the figure, it shows that the fan set with 22.5 mm axial distance between two propellers has the most constant velocity and has a higher velocity at the outlet. Hence, it is selected as the best performance in this section.
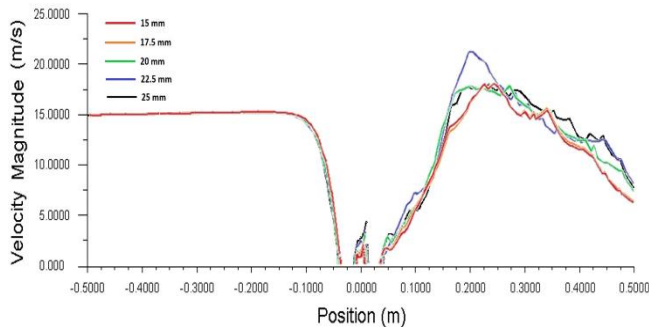

Fig. 8 Centerline velocity for a different set of the distance between two propellers

D. Sound Pressure Level (dB)

The sound pressure level was observed at 3 locations, which were at 50 mm upstream of the first rotor, at the center of the domain, and 0.5 mm downstream from the second rotor. Fig. 9 to 11 shows the sound pressure level for a different distance between two propellers. The highest sound pressure for the point before entering the first propeller appeared at 0.025 Hz, while for between two propellers and after the second propeller appeared at 0.055 Hz. The sound pressure decreases when the frequency increases; it then increases when the frequency reached 0.21 Hz. Next, the 15 mm axial distance between two propellers has the highest sound pressure for the point before entering the first propeller and after the second propeller, which is 57 dB and 53 dB, while the 17.5 mm axial distance between two propellers has the highest sound pressure at the point between two propellers, which is 51 dB.

For the axial distance between two propellers with overall lowest sound pressure, the result showed the 25mm distance between two propellers had the lowest sound pressure at the point before entering the first propeller, which was 55dB, at the point between two propellers which was 46dB and the point after the second propeller which was 52dB. This shows the increase of the distance between two propellers will decrease the value of sound pressure. However, as mention in the previous sub-chapter, due to the limited datasheet, the results are not fully accurate. In this study, the aim is to minimize the noise produce by the fan. Hence, from the figure, it can show that the fan set with 25 mm axial distance between two propellers has produced the least noise in the overall location.
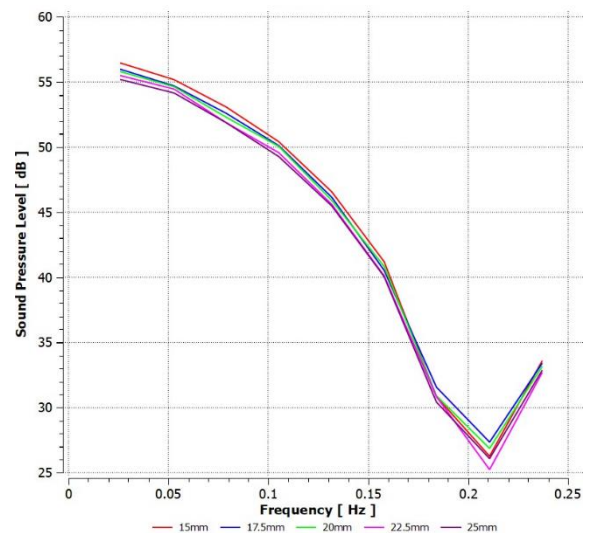

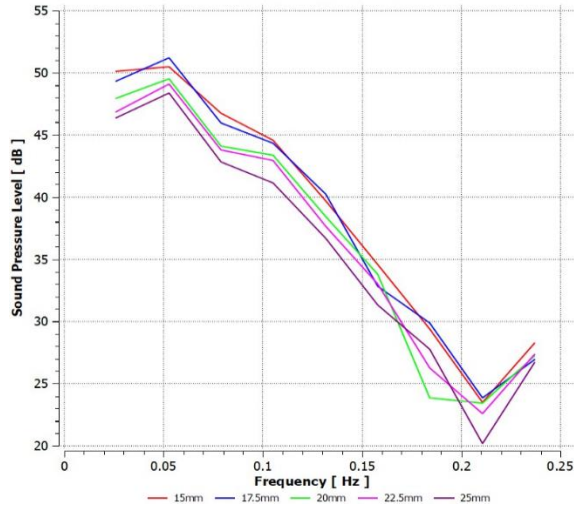**Fig. 9 Sound pressure level at 50 mm upstream of the first rotor**

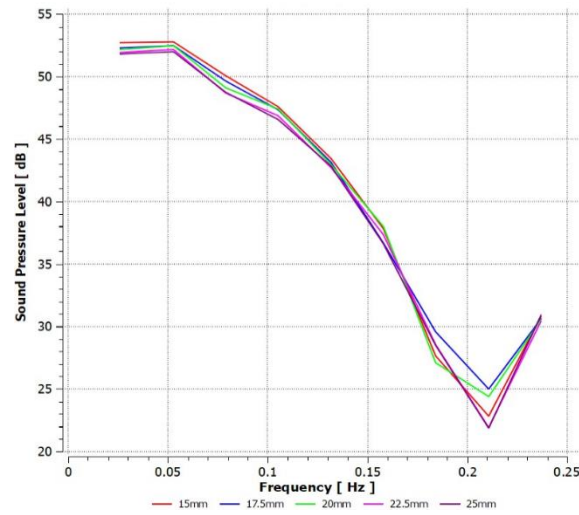**Fig. 10 Sound pressure level at the center of the domain**

Fig. 11 Sound pressure level at 50 mm downstream of the second rotor

E. Broadband Noise Contour

Broadband noise is a noise where its sound energy is distributed over a wide range of frequencies. It is also known as wideband noise, which is opposed to narrowband noise. In this case study, a plane was created at the middle of the domain, as shown in Fig. 12. The reference acoustic power was set to 4e-10 w due to the flow material in the domain is air. The number of realizations was set to 50. Based on the results shown in Fig. 12, the sources of noise produced by the rotors. The second rotor produced higher noise compared to the first rotor. The noise starts to produce when the air flows into the first rotor, which is no noise produced at the area from the inlet to the first rotor. Besides, the rotor hub area also did not produce any noise. The area near to propeller hub produces lower noise than other areas. The highest sound pressure produced among the 5 results is 11 dB, where its axial distance between two rotors was 22.5 mm and 25 mm.

For the axial distance between two propellers 15 mm and 17.5 mm, the highest sound pressure produced in the counter-rotating fan system is 8 dB, while the highest sound pressure for 20 mm axial distance between two propellers is 7 dB. However, this study aims to minimize the noise produce by the fan. Hence, the fan set with a 20 mm axial distance between two propellers, which produce the least noise in overall location, has the best performance in this section.
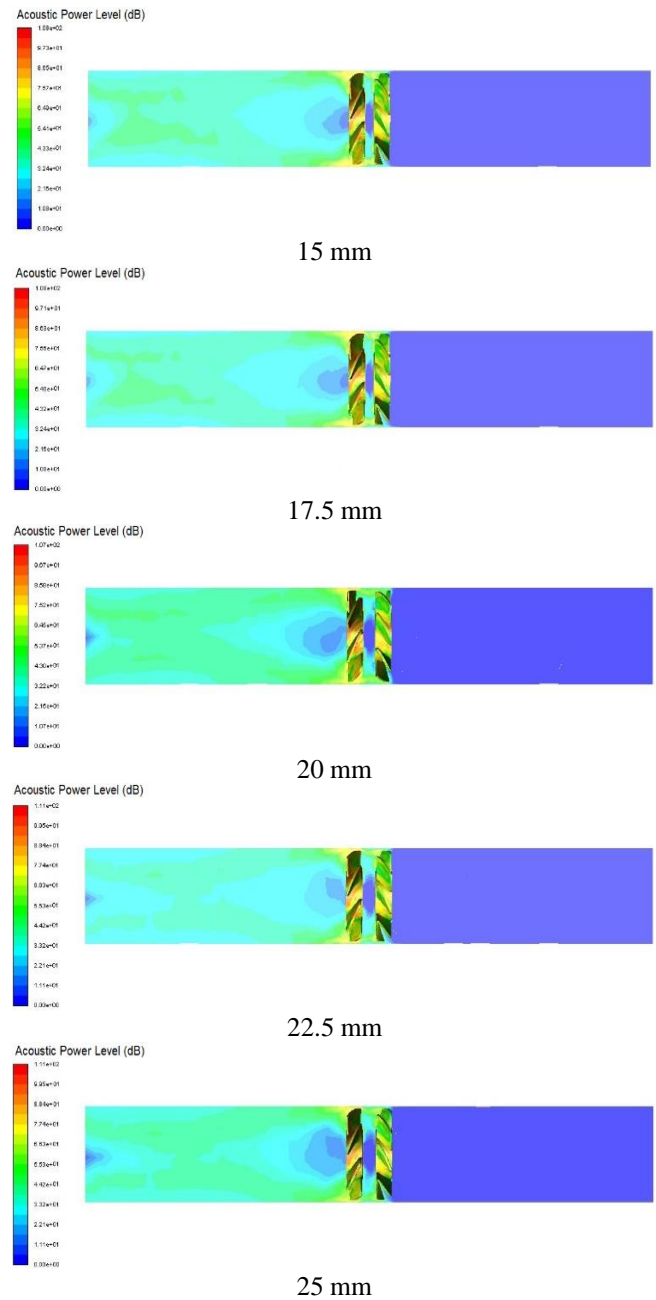

15 mm

17.5 mm

20 mm

22.5 mm

25 mm

Fig. 12 Broadband noise contour for the different distance between two propellers

IV. CONCLUSION

This research is aimed to study the performance of airflow and acoustic behaviour of the contra-rotating fan. The design of the contra-rotating fan was referred to San Ace 172 series counter-rotating fan. The RNG k-ε model was used to contribute to the significate airflow performance of the fan, while the Ffows Williams and Hawkings (FW-H) model was used to contribute to the significate sound pressure level of the fan. Based on the results obtained, the result showed that the increase of the rotating speed would also increase the efficiency of the fan, and the increase of the distance between two rotors also will increase the efficiency of the fan. However, it will be decreased after reaching a maximum distance. Another result obtained from the simulation work is regarding the main noise source of the contra-rotating fan. Based on the results, the noise was increased when the rotating speed of the rotors was increased. However, the noise can be decreased by increasing the distance between two fan sets were increased. In conclusion, it was found that the contra-rotating fan with 20 mm distance between two propellers and rotating with 2000 rpm speed parameters was the most efficient and produced the least noise fan throughout this research. The results agreed very well with the research work from the other researchers. For future study, it was recommended to carry more data for the numerical study. Hence, the result would become more accurate. Besides, more studies on the different types of parameters such as thickness, angle and number of blades, inlet speed, and fan size were suggested.

REFERENCES

[1] Q. G. Chen, W. Sun, F. Li, and Y. J. Zhang, Air-Structure Coupling Features Analysis of Mining Contra-Rotating Axial Flow Fan Cascade, IOP Conf. Series: Materials Science and Engineering, 52 (2013) 022040.

[2] N. Mathan Kumar, C.K. Murugesan, P. Saravanan, Design & Performance Analysis Of Exhaust Fan Blade, SSRG International Journal of Mechanical Engineering 7(4) (2020) 25-28.

[3] R. A. D. Akkermans, M. Pott-Pollenske, H. Buchholz, J. W. Delfs, and D. Almoneit, Installation Effects of a Propeller Mounted on a High-Lift Wing with a Coanda Flap - Part I: Aeroacoustic experiments, in 20th AIAA/CEAS Aeroacoustics Conference (2014) 1-14.

[4] B. Manshoor and A. Khalid, Numerical Investigation of the Circle Grids Fractal Flow Conditioner for Orifice Plate Flowmeters, Applied Mechanics and Materials 229-231 (2012) 700-704.

[5] T. Shigemitsu, J. Fukutomi, Y. Okabe, K. Iuchi, and H. Shimizu, Unsteady Flow Condition of Contra-Rotating Small-Sized Axial Fan, J. Therm. Sci. 20 (2011) 495–502.

[6] H.S. Kadhim, Modeling and Numerical Simulation for the New Design Combined Blades Vertical Axis Wind Turbine, Al-Muhandis Journal 155(2) (2018) 7-13

[7] K.B. Gaywala, H.A. Shah, P.T. Patel, Performance Prediction of a Straight-Bladed Darrieus Water Turbine using Multiple Stream Tube Model, SSRG International Journal of Mechanical Engineering 4(6) (2017) 41-45

[8] I. Zaman, M.M. Salleh, B. Manshoor, A. Khalid and S. Araby, The Application of Multiple Vibration Neutralizers for Vibration Control in Aircraft, Applied Mechanics and Materials 629 (2014) 191-196.

[9] S.G. Zuo, H.U. Qing, H.J. Han, Influence of Blade Thickness on Regenerative Blower's Blade Noise, Journal of Vibration and Shock 33(8) (2014) 130-147.

[10] G. Grasso, J. Christophe, C. Schram, Influence of the Noise Prediction Model on the Aeroacoustic Optimization of a Contra-Rotating Fan. Proceedings of the 20th AIAA/CEAS Aeroacoustics Conference, 2014.

[11] C. Polacsek and R. Barrier, Numerical Simulation of Counter-Rotating Fan Aeroacoustics. AIAA Paper, 2007.

[12] C.X. Li, Q. Lin, X.L. Ding, Performance, Aeroacoustics and Feature Extraction Of An Axial Flow Fan With Abnormal Blade Angle, Energy 103 (2016) 322-339.

[13] J. Wu, Z. Kou, and J. Liu, The Acoustical Behavior of Contra-Rotating Fan, Math. Probl. Eng. 2018 (2018) 3739067.

[14] A. Khalid, et al. Computational Fluid Dynamics Analysis of High Injection Pressure Blended Biodiesel, IOP Conference Series: Materials Science and Engineering 226 (2017) 012002.

[15] Y. Wang, W. Chen, H. Wang, and R. Li, A Computational Study on the Aerodynamics of a 90 mm Ducted Contra-Rotating Lift Fan, Sch. Power Energy, Univ. Northwest. Polytech. Univ, (2016) 126–133.

[16] Y. Wu and D. Huang, Optimization Design of Axial Fan Blade, J. Chinese Inst. Eng. Trans. Chinese Inst. Eng. A, 42(6) (2019) 473–47.

[17] X. Wang, S. Bushan, B. Manshoor, E. Luke, A. Sescu, Y. Hattori, D. Thompson and K. Walters, Dynamic Hybrid RANS/LES Assessment of Sound Generation and Propagation from Flow over a Circular Cylinder, In 2018 AIAA/CEAS Aeroacoustics Conference, AIAA AVIATION Forum, (AIAA 2018-3592), 2018.